Tunable optical delay using photonic crystal heterostructure nanocavities

D. O'Brien,[1,*] A. Gomez-Iglesias,[1] M. D. Settle,[1] A. Michaeli,[2] M. Salib,[3] and T. F. Krauss[1]
[1]*School of Physics and Astronomy, University of St. Andrews, Fife KY16 9SS, United Kingdom*
[2]*Intel Corporation, Kyriat Gat 82109, Israel*
[3]*Intel Corporation, 2200 Mission College Boulevard, Santa Clara, California 95054, USA*
(Received 16 May 2007; published 12 September 2007)

We demonstrate tunable optical delay in a coupled resonator structure consisting of a chain of three heterostructure nanocavities. The group index of the device is measured using an interferometric technique, and the tuning is accomplished by the use of an optical pump that selectively heats one of the cavities in the array, altering the coupling and so changing the delay of the system. The speed of light in the device is varied over a range from $c/75$ to $c/120$ using effective pump powers below 100 μW.

DOI: 10.1103/PhysRevB.76.115110 PACS number(s): 78.67.−n, 42.70.Qs, 42.82.Bq, 42.82.Et

I. INTRODUCTION

Recently, there has been a lot of interest in methods for manipulating and altering the speed of light in different systems, as controlling the speed of light is very desirable for all-optical signal processing functionality as well as quantum optic applications. The three main approaches for achieving "slow light" are through using electromagnetically induced transparency,[1] the slow light region of a photonic crystal waveguide,[2] or coupled resonator structures (CRSs).[3] These three approaches have much in common, as they all use the interaction between different resonances to create suitable conditions for slow light propagation. A detailed comparison may be found in Ref. 4 with the similarities between these different approaches being highlighted in Refs. 5 and 6. Compact optical delay lines with very low dispersion and low group velocity may be achieved in CRSs.[3] Different routes to achieving this in a solid state monolithic device have been explored experimentally using coupled rings[7] and photonic crystal nanocavities.[8,9] Photonic crystals have the advantage that many other optical elements may also be integrated together using this architecture. Mode volumes of photonic crystal nanocavities can also be very small $[\sim(\lambda/2n)^3]$, with greater light-matter interaction, which could be important for nonlinear processes and the possible integration of switching functionality. High sensitivity to fabrication inaccuracies and higher loss are the main limitations of the photonic crystal approach. Despite these difficulties, recent advances in the design and fabrication of photonic crystal nanocavities have led to Q factors $>10^6$, which makes the photonic crystal system appear promising after all. We use one of the types of nanocavities, i.e., the heterostructure design,[10] as the basic building block of a CRS.

In order to understand the physics of this device and explore its potential for tunability, we look at a simple system consisting of just three coupled heterostructure nanocavities. Although photonic crystal channel waveguides can provide slow light propagation over a greater bandwidth,[2] it is as yet not possible to tune the delay of these devices. By tuning the individual cavities of a CRS, however, such tuning is indeed possible, which allows us to present a demonstration of group velocity tuning in a photonic crystal system. Pumping with modest power levels ($\sim$100 μW) induces a sufficient change in the refractive index of the nanocavity to tune it significantly. This alters the bandwidth of the coupled system, thereby modifying the delay experienced by light traveling through the CRS and providing the principle of operation for a tunable optical delay line. Please note that, ideally, the transfer function of the CRS should have a "top-hat-like" characteristic, with the peaks corresponding to the individual cavities not being discernible. Such a characteristic can be achieved via suitable apodization, which will be implemented in due course; at this stage, it helps the interpretation of the results, however, if the individual peaks can be identified.

The behavior of an infinitely long CRS in a given material system may be defined by the coupling constant between the cavities (t) and the distance between the cavities (d). The dispersion relation has a cosine nature and may be written as

$$\cos(\beta d) = \frac{\sin(kd)}{t}, \tag{1}$$

where β is the phase constant of the propagating wave and k is the wave vector inside each resonator. The amplitude of the oscillation and the bandwidth of the system are determined by the coupling constant t:

$$B = \frac{c}{n_0 d\pi}\sin^{-1}(t), \tag{2}$$

n_0 being the waveguide linear effective index. From the slope of the dispersion relation, the group velocity for the CRS state can be written as

$$v_g = \mp\frac{c}{n_0}\frac{\sqrt{t^2-\sin^2(kd)}}{\cos(kd)}. \tag{3}$$

Although the above analysis is for an infinitely long CRS, these relations also give insight into finite length structures, even those consisting of just a few cavities. For example, the size of the mode splitting associated with just two coupled cavities is very close to the bandwidth as calculated for an infinite CRS. The above relations can therefore be used to gain an intuitive understanding of these devices. From Eqs. (2) and (3), the bandwidth and group velocity are intimately related and can be controlled by the coupling between the

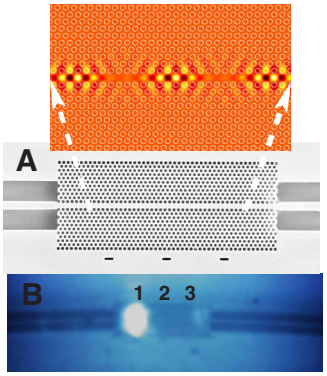

FIG. 1. (Color online) Top: Calculated electric field profile of a three cavity system. (A) SEM image of the input and output ridge waveguides and photonic crystal containing three cavities. (B) The same device as seen through an optical microscope. The spot from the vertical pump is seen on cavity 1 of the CRS.

cavities, t. Weaker coupling leads to lower bandwidth and lower group velocity, and vice versa.

II. TRANSMISSION EXPERIMENT

The devices were fabricated on silicon on insulator wafers with a 240 nm Si layer on top of 2 μm buried oxide.[2] A window was defined over the photonic crystal area to selectively remove the SiO_2 layer underneath with HF, while the ridge waveguide remains supported by the unetched SiO_2. The device design comprises a series of heterostructure cavities[10] separated by nine rows of holes. The devices had a lattice constant of 420 nm, which sets the distance between different cavities $d \sim 5$ μm. A ridge waveguide was used to couple light to and from the CRS. Images of the devices from an optical microscope and a scanning electron microscope (SEM) are shown in Fig. 1.

Devices were cleaved and then probed using an amplified spontaneous emission source with a bandwidth of 50 nm in an end fire arrangement along the ridge waveguide. The resulting transmission was collected and analyzed in an optical spectrum analyzer (0.01 nm resolution). The Q factor for a single cavity was measured as 10 000. For the coupled cavity system, a splitting of the optical modes of 1 nm was observed, which indicates that the overall cavity Q factor is limited by out-of-plane losses. With the addition of further cavities, additional mode splitting causes the bandwidth of the defect state to become populated.[9]

In order to tune the system, an additional laser diode operating at 850 nm was used as an optical pump and focused down vertically onto the photonic crystal structure. Imaging and vertical pumping of the photonic crystal structure was performed through the same optical microscope. The vertical pump was focused to give an $\sim 5 \times 10$ μm^2 elliptical spot. This was then used to selectively pump the photonic crystal, addressing each cavity separately. The power level of the pump beam as focused onto the sample was varied up to 20 mW. In order to estimate the amount of power that is absorbed by the cavities, we must take into account the reflection at the air/semiconductor interface (30%) and the fraction absorbed by Si at a wavelength of 850 nm across a 240 nm thick Si slab (0.8%). Light that is transmitted through the slab is absorbed by the Si substrate, which is thermally isolated by the air gap from the CRS membrane. With these factors considered, the amount of power that is absorbed by the material is ~ 100 μW. This power level is comparable to that required for thermally tuning a photonic crystal Mach-Zehnder device[11] (~ 1 mW), when taking the respective size differences into account. The transmission spectra of the devices were analyzed for different levels of this vertical pump power. The transmission results are presented in Fig. 2.

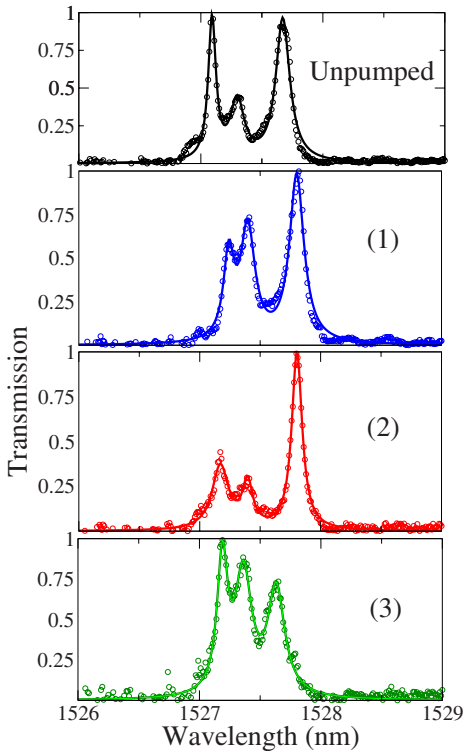

FIG. 2. (Color online) Lorentzian fits to transmission spectra of the unpumped CRS and while pumping cavities 1, 2, and 3 of the CRS. In this case, pumping cavity 3 decreased the bandwidth of the CRS band.

Lorentzian line shapes were fitted to the three peaks of the transmission spectra, which allows us to trace the reordering of the peaks that we observed for the different pumping conditions. The bandwidth of the system is affected either by shrinking or extending the mode splitting, depending on the specific cavity being addressed and the vertical pump power level being used. The tuning of the peaks as found through the fitting procedure was seen to be linear over the range of pump levels explored. We observed that the bandwidth of the system may either increase or decrease with increasing pump power (Fig. 3) and that the transmission spectrum with the lowest bandwidth has peaks that are more equally spaced (Fig. 2). Both the decreasing bandwidth with tuning in one case and the unequally spaced peaks in the unpumped case indicate that the cavities are not perfectly on resonance due

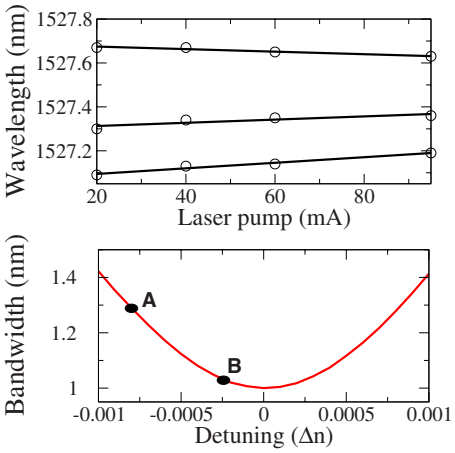

FIG. 3. (Color online) Top: The positions of the mode peaks were found by fitting Lorentzians to the experimental transmission spectra for different pump powers when pumping the rightmost cavity. A linear tuning of up to 25% of the CRS bandwidth is observed. Bottom: Inducing a change in refractive index (Δn) by as little as 6.5×10^{-4} in the cavity, the calculated bandwidth of the CRS may be altered by 25%. Tuning from points A to B illustrates this range.

to limitations in the fabrication process, i.e., they experience an element of "prebiasing" in terms of bandwidth.

In order to understand these results, the response of the coupled cavity system was modeled using a one dimensional transfer matrix approach[12] for the different pumping conditions. The optical pumping is modeled as a local change in the refractive index of the material in a given cavity. The bandwidth of the system has a parabolic dependence on detuning with a minimum for the resonance condition of zero detuning, as shown in Fig. 3. The bandwidth of the system is set by the coupling coefficient between the different cavities (t) as shown in Eq. (2). The equation assumes perfect agreement of all the cavity resonances. If individual cavities are detuned, the bandwidth of the system increases due to the phenomenon of "inhomogeneous broadening" that is well known from atomic systems.

As the bandwidth is observed to decrease with increasing tuning for certain cases, we may conclude that our system is not initially exactly on resonance. As the tuning behavior (Fig. 3, bottom) is also parabolic close to the point of resonance, the almost linear tuning curves observed experimentally (Fig. 3, top) further indicate that the system operates away from perfect resonance. For the purposes of altering the bandwidth of the CRS, this may, in fact, be advantageous as it is better to be operating slightly off resonance to get a larger change in bandwidth for a given amount of detuning. The index shift required to achieve the observed change in bandwidth is calculated to be 6.5×10^{-4}. It is worth noting that this level of detuning is significantly smaller than the wavelength splitting caused by intercavity coupling; in other words, the inhomogeneous broadening is smaller than the homogeneous broadening. As the detuning approaches the splitting, the cavities decouple and the system no longer behaves as a CRS, which would require stronger detuning than realized here.

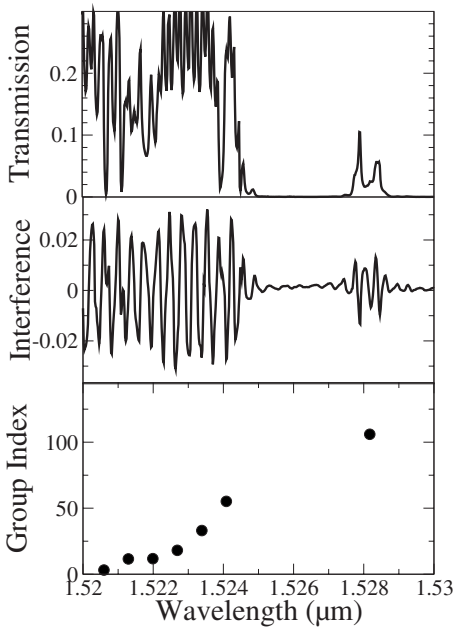

FIG. 4. Transmission, interferogram, and extracted value for group index for the unpumped case in Fig. 2. This spectral region contains both the end of the W1 passband (1.5245 μm) and the CRS defect state (1.528 μm). The calculated group index values are an average of the group index over the spectral width of the defect state.

III. DELAY RESULTS

From Eq. (3), a shrinking or expanding of the bandwidth should be accompanied by a change in the group velocity of the light as it passes through the device. In order to investigate the effect on the group index ($n_g=c/v_g$) of the CRS of changing the bandwidth, we used a spectral interferometric technique combined with Fourier transform analysis.[13] Similar interferometric methods were recently used in all monolithic structures to estimate the group velocity of light in photonic crystals.[11,14]

The same apparatus used for the transmission measurements was placed in one arm of a Mach-Zehnder interferometer (MZI), whose output yields interference fringes of a period inversely proportional to the optical path difference between the two arms (the phase shift between two adjacent maxima of the oscillations is 2π, as they correspond to constructive interference). This fringe pattern is resolved in a single shot by an optical spectrum analyzer, and separate spectra of the sample and reference arms are taken to subtract the noninterfering background (see the middle graph in Fig. 4 for an example). A delay stage in the reference arm is used to initially set the path difference so that the spacing between fringes close to the cutoff of the W1 passband and CRS modes can be easily resolved (note that the stage is kept fixed during the measurements and no mechanical delay scan is required). Also, the intensity in the reference arm is adjusted to optimize the visibility of the interference pattern. A Fourier transform is performed on the background-free interferogram. In the time domain, due to the carefully chosen optical path imbalance between the MZI arms, the two

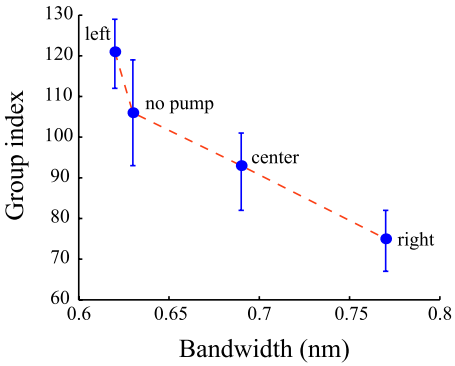

FIG. 5. (Color online) Group index versus bandwidth for a number of different pumping conditions. Each data point was extracted from transmission spectra like those presented in Fig. 4.

crossed complex interference terms appear shifted and one of them can be filtered numerically. Then, by applying an inverse Fourier transform, the phase shift between the two arms can be extracted. For each of the four pumping scenarios, the corresponding difference in group delay was obtained by differentiating this phase shift with respect to frequency. An additional measurement without the device in the MZI was used to calibrate the setup and thus obtain the group indices in the sample at different wavelengths. Typical transmission spectra along with the extracted group index are shown in Fig. 4. The fringe spacing in the interferogram is set by the relative path difference of the two arms of the Mach-Zehnder interferometer. For the short devices measured, the contribution to the overall delay of the Mach-Zehnder interferometer is small. As such, the variation in fringe spacing in the interferogram due to the change in group index of the device is not easily visible before data analysis. For longer devices, where the delay introduced by the device is more significant with regard to the total delay of the arm, a clearer variation of fringe spacing as the group index changes is observable.[14]

The group index rises as expected with decreasing bandwidth, as shown in Fig. 5. As discussed previously, this is due to the fact that the slight disorder initially present in the system is reduced (case left); conversely, the group index decreases when increasing the disorder in the system (case right), which also agrees with other studies on the effect of disorder in CRS.[15] The refractive index of silicon changes with temperature[16] as $\Delta n_\theta = \kappa_\theta \Delta T$, where $\kappa_\theta = 1.86 \times 10^{-4}$ K^{-1}. In the devices explored here, the change in temperature required to bring about a change in refractive index of 6.5×10^{-4} is 3.5 K. The relationship between the temperature change and absorbed power may be written[17] as

$$\frac{d\Delta T}{dt} + \frac{\Delta T}{\tau_\theta} = -\frac{P}{\rho C V}, \tag{4}$$

where ΔT is the temperature change, $\tau_\theta (=1\ \mu s)$ is the thermal dissipation time, and P is the absorbed optical power. $\rho (=2.3 \times 10^{-3}$ kg/cm$^3)$ and $C (=705$ J kg^{-1} K$^{-1})$ are, respectively, the density and thermal capacity of silicon. For a steady state condition with a cw probe, the absorbed optical power may be written as

$$P = -\frac{\Delta T \rho C V}{\tau_\theta}. \tag{5}$$

Taking the volume $V \approx 5\ \mu m \times 10\ \mu m \times 240$ nm and substituting this into Eq. (5), the pump power required to achieve the estimated temperature change of 3.5 K is 75 μW. This is in good agreement with our experimental estimate of absorbed power.

IV. CONCLUSION

We present a demonstration of actively tuning the group velocity in a photonic crystal using three coupled defect resonators. The effect of different tuning conditions is explored and a tuning range from +15% to −40% in group index is demonstrated. This tuning range is achieved using modest effective power levels of around 100 μW. The effect of prebiasing the coupled resonator structure is discussed, which enables us to both decrease and increase the group velocity with tuning.

ACKNOWLEDGMENT

The authors would like to acknowledge Tim Karle for his help in the construction of the experiment.

*do10@st-andrews.ac.uk

[1] C. Li, Z. Dutton, C. Behroozi, and L. Hau, Nature (London) **409**, 490 (2001).
[2] M. Settle, R. Engelen, M. Salib, A. Michaeli, L. Kuipers, and T. Krauss, Opt. Express **15**, 219 (2007).
[3] A. Yariv, Y. Xu, R. K. Lee, and A. Scherer, Opt. Lett. **24**, 711 (1999).
[4] J. B. Khurgin, J. Opt. Soc. Am. B **22**, 1062 (2005).
[5] Z. Wang and S. Fan, Phys. Rev. E **68**, 066616 (2003).
[6] T. Krauss, J. Phys. D **40**, 2666 (2007).
[7] F. Xia, L. Sekaric, and Y. Vlasov, Nat. Photonics **1**, 65 (2007).
[8] T. Karle, Y. Chai, C. Morgan, I. White, and T. Krauss, J. Lightwave Technol. **22**, 514 (2004).
[9] D. O'Brien, M. Settle, T. Karle, A. Micaheli, M. Salib, and T. Krauss, Opt. Express **15**, 1228 (2007).
[10] B. S. Song, S. Noda, T. Asano, and Y. Akahane, Nat. Mater. **4**, 207 (2005).
[11] Y. Vlasov, M. Boyle, H. Hamann, and S. McNab, Nature (London) **438**, 65 (2005).
[12] E. Hecht, *Optics*, 4th ed. (Addison-Wesley, New York, 2002).
[13] M. Takeda, H. Ina, and S. Kobayashi, J. Opt. Soc. Am. **72**, 156 (1982).
[14] A. Gomez-Iglesias, D. O'Brien, L. O'Faolain, A. Miller, and T. Krauss, Appl. Phys. Lett. **90**, 261107 (2007).
[15] S. Mookherjea and A. Oh, Opt. Lett. **32**, 289 (2007).
[16] G. Cocorullo and I. Rendina, Electron. Lett. **28**, 83 (1992).
[17] Q. Xu and M. Lipson, Opt. Lett. **31**, 341 (2006).